JCB Article

Myosin-II reorganization during mitosis is controlled temporally by its dephosphorylation and spatially by Mid1 in fission yeast

Fumio Motegi,[1,2] Mithilesh Mishra,[3] Mohan K. Balasubramanian,[3] and Issei Mabuchi[1]

[1]Division of Biology, Department of Life Sciences, Graduate School of Arts and Sciences, University of Tokyo, Tokyo, 153-8902, Japan
[2]Center for Developmental Biology, RIKEN, Kobe, 650-0047, Japan
[3]Temasek Life Sciences Laboratory, The National University of Singapore, 117604, Singapore

Cytokinesis in many eukaryotes requires an actomyosin contractile ring. Here, we show that in fission yeast the myosin-II heavy chain Myo2 initially accumulates at the division site via its COOH-terminal 134 amino acids independently of F-actin. The COOH-terminal region can access to the division site at early G2, whereas intact Myo2 does so at early mitosis. Ser1444 in the Myo2 COOH-terminal region is a phosphorylation site that is dephosphorylated during early mitosis. Myo2 S1444A prematurely accumulates at the future division site and promotes formation of an F-actin ring even during interphase. The accumulation of Myo2 requires the anillin homologue Mid1 that functions in proper ring placement. Myo2 interacts with Mid1 in cell lysates, and this interaction is inhibited by an S1444D mutation in Myo2. Our results suggest that dephosphorylation of Myo2 liberates the COOH-terminal region from an intramolecular inhibition. Subsequently, dephosphorylated Myo2 is anchored by Mid1 at the medial cortex and promotes the ring assembly in cooperation with F-actin.

Introduction

Cells must assure correct spatial and temporal coordination of mitosis with cytokinesis so that each daughter cell will receive proper genetic materials and cellular components. In eukaryotes, cytokinesis requires assembly of the actomyosin-based contractile ring (CR) at the cell cortex where cell division takes place. However, molecular mechanisms of positioning of the division plane and following assembly of the CR have been poorly understood.

Myosin-II, hereafter referred to as myosin, is believed to be a molecular motor that generates force for cytokinesis by interacting with actin filaments at the CR. The myosin molecule consists of a pair of heavy chains and two pairs of light chains. Each heavy chain has an NH_2-terminal motor domain and a long α-helical tail that allows the molecules to assemble into bipolar filaments. Recently, several lines of evidence have suggested that myosin localizes at the division site independently of actin filaments. Mutated myosin defective in binding with actin filaments still accumulates at the division site in *Dictyostelium discoideum* cells (Zang and Spudich, 1998) and fission yeast cells (Naqvi et al., 1999). Myosin localization at the CR is maintained in the absence of actin filaments in isolated cleavage furrow of sea urchin egg (Schroeder and Otto, 1988), budding yeast cells (Bi et al., 1998), and fission yeast cells (Naqvi et al., 1999). Furthermore, accumulation of myosin at the division site appears to occur earlier than that of actin filaments in budding yeast cells (Lippincott and Li, 1998), fission yeast cells (Motegi et al., 2000), and *Xenopus laevis* egg (Noguchi and Mabuchi, 2001). However, it is unclear how myosin is targeted to the division site.

The fission yeast *Schizosaccharomyces pombe* is an attractive model system to study the coordination of mitosis with cytokinesis. The cylindrical *S. pombe* cells undergo symmetrical division using a medial CR as in higher eukaryotes (for review see Le Goff et al., 1999). The CR assembles during mitosis before nuclear division is achieved, and then contracts during septation (Marks and Hyams, 1985; Kitayama et al., 1997). Position of the nucleus, not the mitotic spindle, may determine the site for formation of the CR (Chang and

Address correspondence to Issei Mabuchi, Division of Biology, Graduate School of Arts and Science, University of Tokyo, Komaba, Meguro-ku, Tokyo 153-8902, Japan. Tel.: 81-3-5454-6630. Fax: 81-3-5454-4318. email: mabuchi@ims.u-tokyo.ac.jp

Key words: myosin; actin; phosphorylation; cytokinesis; contractile ring

Abbreviations used in this paper: CR, contractile ring; NETO, new end take off.

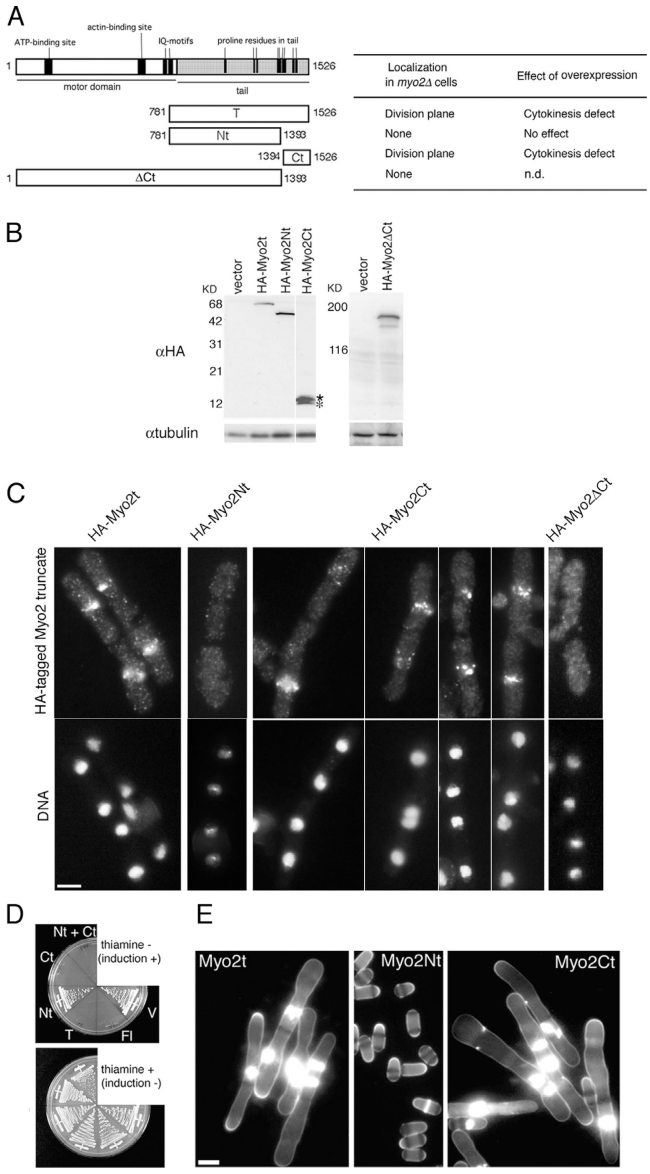

Figure 1. **COOH-terminal 134 aa of Myo2 is crucial for accumulation at the division site and for inducing the cytokinesis defect.** (A) Schematic diagram of Myo2 and those of Myo2 truncates. Localization of these truncates expressed in *myo2*Δ cells and effect of overexpression of these truncates in wild-type cells are also shown. (B) Immunoblotting of extracts from cells expressing truncates of Myo2. Diploid cells (*myo2*$^+$/*myo2::ura4*$^+$) carrying constructs for the expression were grown in the medium containing thiamine, and then transferred into the medium without thiamine for 20 h. Extracts were prepared and analyzed by SDS-PAGE followed by immunoblotting using anti-HA antibodies (top) and anti–α-tubulin antibodies (bottom). Top asterisk indicates a slower migrating HA-Myo2Ct and bottom asterisk indicates a faster migrating one. White line indicates that intervening lanes have been spliced out. (C) Localization of Myo2 truncates in *myo2*Δ cells. Diploid cells (*myo2*$^+$/*myo2::ura4*$^+$) expressing the Myo2 truncates were induced to undergo meiosis in a liquid medium. Spores were isolated and inoculated into a medium where only those bearing both the *myo2::ura4*$^+$ allele and the constructs could germinate. Germinating spores were fixed and stained simultaneously with anti-HA antibodies (top) and DAPI (bottom). White lines indicate that intervening lanes have been spliced out. Bar, 3.3 μm. (D) Growth of wild-type cells carrying construct for expression of HA-Myo2 (Fl), HA-Myo2t (T), HA-Myo2Nt (Nt), HA-Myo2Ct (Ct), both HA-Myo2Nt and HA-Myo2Ct (Nt + Ct), or empty vector (V). These cells were grown at 30°C on a plate without thiamine (top) or that containing thiamine (bottom). (E) Effects of overexpression of Myo2 truncates on cell morphology and septum formation. Cells carrying the constructs were grown at 30°C for 20 h in the absence of thiamine, and then stained with Calcofluor. Bar, 3.3 μm.

Nurse, 1996; Chang et al., 1996). Several genes involved in proper placement of the CR have been identified, including *mid1*/*dmf1* (Chang et al., 1996; Sohrmann et al., 1996) and *plo1* (Bahler et al., 1998). Mid1 localizes at both nucleus and medial cortex overlying the nuclei during interphase, suggesting that Mid1 may function as a molecular link that positions the CR near the nucleus (Sohrmann et al., 1996; Paoletti and Chang, 2000). The Polo kinase Plo1 appears to have a role in regulating the behavior of Mid1 probably by phosphorylation (Bahler et al., 1998). However, little is known about how Mid1 and Plo1 promote reorganization of the actin cytoskeleton during early mitosis.

The fission yeast has two myosin heavy chains, Myo2 and Myp2/Myo3 (Benzanilla et al., 1997; Kitayama et al., 1997; May et al., 1997; Motegi et al., 1997), both of which localize at the CR during cytokinesis. Myo2 is essential for viability of the cell and cytokinesis, whereas Myp2/Myo3 is required for cytokinesis under certain conditions. We have previously shown that Myo2 assembly into the CR consists of two steps (Motegi et al., 2000). Myo2 initially accumulates as multiple dots at the medial cortex independently of F-actin. Subsequently, these Myo2 dots are converted into filamentous structures, and then coalesce into a ring in a manner dependent on F-actin. The latter step also requires motor activity of Myo2 (Naqvi et al., 1999) and function of Rng3, a protein containing a UCS domain that is thought to be a molecular chaperon for myosin (Wong et al., 2000; Barral et al., 2002).

In this paper, we focused on the mechanism of initial accumulation of Myo2 at the division site. We identified the minimum sequence of Myo2 that is both necessary and sufficient for the accumulation. Our data suggest that the accumulation of Myo2 is coordinated with mitosis through dephosphorylation at S1444 of Myo2. Mid1 anchors dephosphorylated Myo2 at the cortex overlying the nucleus, and then the cortical Myo2 promotes assembly of the CR in cooperation with F-actin.

Results

A COOH-terminal region of Myo2 is necessary and sufficient for the accumulation at the division site

In *S. pombe* cells, truncated myosin that lacks the motor domain accumulates at the division site (Naqvi et al., 1999; Mulvihill et al., 2001). To identify a specific sequence of Myo2 for the accumulation, we examined localization of a series of truncated Myo2 in *myo2* null (*myo2*Δ) cells. Although Myo2 tail appears to be entirely α-helical, the sequence predicts presence of a gap due to a cluster of proline residues at 1390–1400 aa (Benzanilla and Pollard, 2000). Thus, we constructed a series of truncates cut apart at the gap (Fig. 1 A): entire tail (Myo2t, 781–1526 aa), NH_2-terminal region of the tail (Myo2Nt, 781–1393 aa), COOH-terminal region of the tail (Myo2Ct, 1394–1526 aa), and

Myo2 lacking the Myo2Ct region (Myo2ΔCt, 1–1393 aa). Localization of each truncate tagged at the NH_2 terminus with HA epitope was observed in the *myo2*Δ cells. Expression of the HA-tagged truncate was confirmed by immunoblotting (Fig. 1 B). Either HA-Myo2t or HA-Myo2Ct was found as multiple dots at the cortex between segregating nuclei, which is the expected division site (Fig. 1 C). In contrast, neither HA-Myo2Nt nor HA-Myo2ΔCt showed any specific localization in these cells (Fig. 1 C). Truncated HA-Myo2Ct that lacked 10 aa from either NH_2- or COOH-terminal did not accumulate at the division site (unpublished data). These results indicate that the Myo2Ct region is necessary and sufficient for the accumulation in the absence of the wild-type protein.

Overexpression of Myo2Ct specifically inhibits formation of the CR

Next, we examined phenotype of cells overexpressing the Myo2 truncates. Each construct for expression of the HA-tagged Myo2 truncate under the *nmt1* thiamine repressible promoter (Maundrell, 1989) was transformed into the wild-type strain. All the transformants grew well on a plate containing thiamine. However, in the absence of thiamine cells carrying the construct for HA-Myo2, HA-Myo2t, HA-Myo2Ct, or both HA-Myo2Nt and HA-Myo2Ct failed to form colonies, whereas those carrying the construct for HA-Myo2Nt or empty vector grew well (Fig. 1 D). Cells overexpressing either HA-Myo2t or HA-Myo2Ct were elongated due to a defect in cytokinesis, whereas cells overexpressing HA-Myo2Nt showed a normal morphology (Fig. 1 D). These results indicate that expression of the Myo2Ct region causes failure in cytokinesis.

To further investigate effects of HA-Myo2Ct expression on cytokinesis, we examined distribution of F-actin during the first mitosis after increase of the expression. The *cdc25-22* temperature-sensitive mutant cells arrest cell cycle at G2 in the absence of Cdc25 activity, and restoring the activity results in rapid commitment to mitosis. Thus, *cdc25-22* cells expressing HA-Myo2Ct were arrested at G2 by temperature shift from the permissive temperature 25°C to the restrictive temperature 37°C. The resultant cells were released by shifting to 25°C. Progression of nuclear division in these cells was similar to that in control cells (Fig. 2 B). F-actin distribution in G2 cells expressing HA-Myo2Ct was similar to that of control G2 cells; F-actin patches were concentrated at both cell ends, and F-actin cables were oriented along the long axis of the cell (Fig. 2 A). 50 min after release from the G2 arrest, 79% of mitotic cells expressing HA-Myo2Ct formed a spot of F-actin from which F-actin cables emanated like aster at the medial region, whereas 82% of mitotic cells carrying empty vector formed a well-defined ring of F-actin at the medial cortex (Fig. 2, A and C). A ring structure of F-actin was never observed through mitosis in the HA-Myo2Ct–expressing cells. Components of the CR, both endogenous Myo2 and Cdc4, accumulated at the aster/spot structure along with F-actin (unpublished data), suggesting that this structure represents an abnormal-shaped CR or a precursor of the CR. These results indicate that expression of Myo2Ct specifically inhibits CR formation.

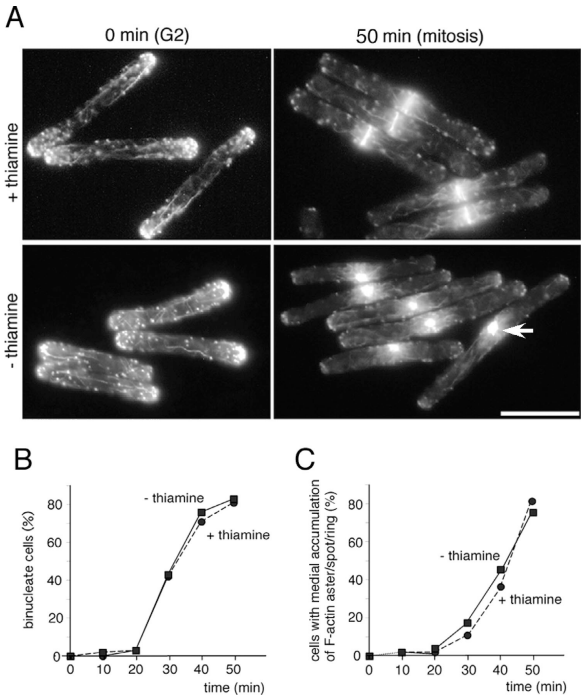

Figure 2. **Ectopic expression of Myo2Ct inhibits formation of the CR.** Effects of HA-Myo2Ct overexpression on F-actin organization (A and C) and progression of nuclear division (B) during G2 and mitosis. *cdc25-22* cells carrying empty vector or construct for expression of HA-Myo2Ct were cultured at 25°C in medium containing thiamine, and then transferred to the medium without thiamine. 12 h after the removal of thiamine, the cells were shifted to 37°C for 3.5 h to arrest cell cycle at G2. A half of the culture was maintained at 37°C, while the other was returned to 25°C for 50 min. The cells were fixed and stained simultaneously for DNA and F-actin. Progression of nuclear division and medial accumulation of F-actin aster, spot, or ring were analyzed at 10-min intervals after the return to 25°C. Arrow indicates a spot/aster structure. Bar, 10 μm.

Myo2Ct accumulates at the division site during early G2, whereas either Myo2 or Myo2t accumulates there during mitosis

Next, we examined localization of Myo2 truncates containing the Myo2Ct region in synchronized *cdc25-22* cells. Either the cells expressing HA-Myo2Ct or those expressing HA-Myo2t were arrested at G2 and released as described in the previous section. Interestingly, HA-Myo2Ct accumulated as multiple dots at the medial cortex in the G2 cells, whereas HA-Myo2t showed no specific localization in these cells (Fig. 3 A). 30 min after the release from G2 arrest, either HA-Myo2Ct or HA-Myo2t was found as multiple dots at the medial cortex where F-actin formed a spot/aster structure (Fig. 3 A). HA-Myo2Ct was also observed at the future division site in asynchronous wild-type cells expressing HA-Myo2Ct (50% of total cells and 72% of interphase cells; Fig. 3, B and D). HA-Myo2Ct was observed at the medial cortex of the G2 cells that coexpressed HA-Myo2Nt (Fig. 3 C), indicating that the coexpression of HA-Myo2Nt did not inhibit the accumulation of HA-Myo2Ct.

To determine the cell cycle stage at which HA-Myo2Ct accumulates at the future division site, we analyzed kinetics of HA-Myo2Ct localization through the cell cycle (Fig. 3

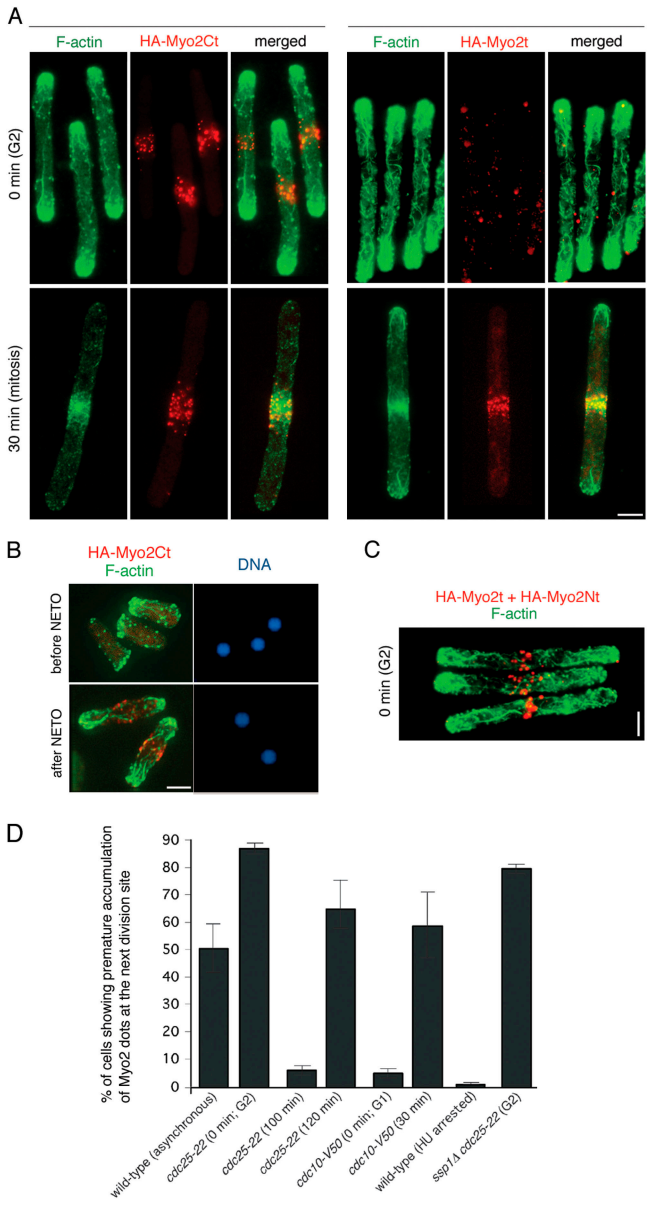

Figure 3. **Localization of Myo2 truncates during interphase.** (A) Localization of the Myo2 truncates in G2 cells (top) or mitotic cells (bottom). *cdc25-22* cells carrying construct for expression of HA-Myo2Ct (left) or HA-Myo2t (right) were simultaneously induced for 16 h and synchronized at G2. A half of the culture was maintained at 37°C, while the other was returned to 25°C for 30 min. The cells were fixed and stained simultaneously with Bodipy-phallacidin (green) and anti-HA antibodies (red). (B) Localization of HA-Myo2Ct in cells before NETO and cells after NETO. Asynchronous wild-type cells expressing HA-Myo2Ct were fixed and stained simultaneously with Bodipy-phallacidin (green), anti-HA antibodies (red), and DAPI (blue). Images of DNA staining indicate that these cells were in interphase. (C) Localization of HA-Myo2Ct in cells overexpressing HA-Myo2Nt. *cdc25-22* cells carrying both construct for expression of HA-Myo2Ct and that of HA-Myo2Nt were grown as in A. The G2-arrested cells were fixed and stained simultaneously with Bodipy-phallacidin (green) and anti-HA antibodies (red). Bars, 3.3 μm. (D) Premature accumulation of HA-Myo2Ct at various cell cycle stages. *cdc25-22* cells expressing HA-Myo2Ct, *cdc10-V50* cells expressing HA-Myo2Ct, or *ssp1*Δ *cdc25-22* cells expressing HA-Myo2Ct were synchronized at various stages of the cell cycle by temperature shift. Times indicate those after the release. Asynchronous wild-type cells and wild-type cells treated with hydroxyurea were also prepared. These cells were fixed and stained simultaneously for HA-Myo2Ct and F-actin. At least 50 cells were examined for each strain under the specified condition and mean values ($n = 3$) are plotted.

D). First, the *cdc25-22* cells expressing HA-Myo2Ct were synchronized at various cell cycle stages by release from the G2 arrest. From 100 to 120 min after the release, when most cells had completed previous cell division, HA-Myo2Ct was found at the future division site in a significant population (65%) of the daughter cells. Next, we observed localization of HA-Myo2Ct in synchronized *cdc10-V50* cells by release from the G1 arrest (Mitchison and Nurse, 1985). The cells expressing HA-Myo2Ct at G1 showed no specific localization of HA-Myo2Ct (Fig. 3 D). At 30 min after the release, HA-Myo2Ct was predominantly found at the next division site (Fig. 3 D). HA-Myo2Ct was not observed at the medial region in hydroxyurea-treated cells in which DNA synthesis was arrested (Fig. 3 D, HU arrested). Transition of distribution of F-actin patches from mono- to bipolar fashion (new end take off [NETO]) has been shown to occur during early G2 (Mitchison and Nurse, 1985). To investigate if NETO is required for the premature accumulation of HA-Myo2Ct, we first observed localization of both F-actin patches and HA-Myo2Ct in asynchronous wild-type cells. The advanced accumulation of HA-Myo2Ct was observed in interphase cells showing bipolar distribution of F-actin patches, but not in cells showing monopolar distribution of F-actin patches (Fig. 3 B). Then, we observed HA-Myo2Ct localization in NETO-deficient mutant *ssp1*Δ cells (Rupes et al., 1999). In G2-arrested *ssp1*Δ *cdc25-22* cells, HA-Myo2Ct predominantly accumulated at the future division site (Fig. 3 D). These results indicate that Myo2Ct prematurely accumulates at the future division site during early G2 in a manner independent of NETO.

Dephosphorylation of S1444 in Myo2 is involved in temporal control of the Myo2 accumulation at the division site

Immunoblotting on extracts from asynchronous cells expressing HA-Myo2Ct showed that anti-HA antibodies recognize two closely migrating bands of ~13–15 kD on SDS-PAGE (Fig. 1 B). Both bands increased after prolonged expression (unpublished data) but were absent in extracts from wild-type cells (Fig. 1 B). Treatment of immunoprecipitated HA-Myo2Ct with alkaline phosphatase reduced the amount of the slower migrating component but increased that of the faster migrating one, whereas treatment with inactivated phosphatase did not affect the band pattern (Fig. 4 A). These results suggest that the slower migrating band represents phosphorylated forms of HA-Myo2Ct. The Netphos 2.0 program estimated that five amino acid residues in Myo2Ct have a probability (>0.5) of sites for phosphorylation: these are T1400, S1444, S1472, S1505, and S1518. To identify the residue that contributes to the mobility change of HA-Myo2Ct, each of these residues was replaced with alanine to mimic a dephosphorylated form. Extracts from cells expressing each mutated HA-Myo2Ct were analyzed by immunoblotting. Of these mutated HA-Myo2Cts, only HA-Myo2Ct S1444A migrated at the position of the

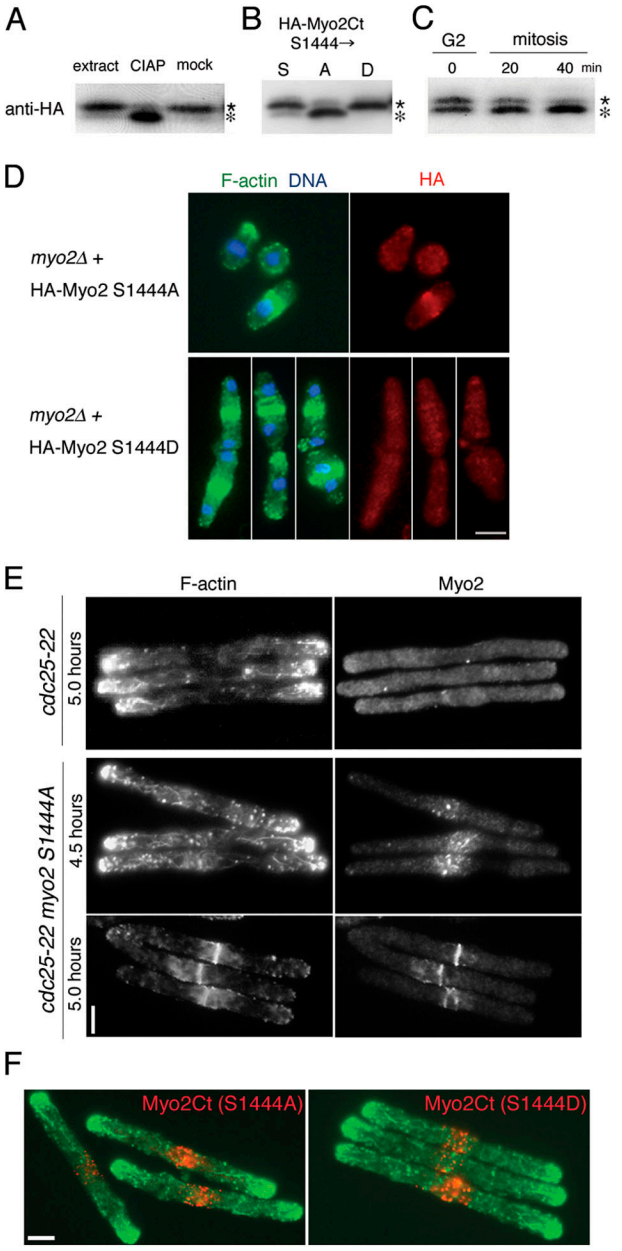

Figure 4. **Role of S1444 phosphorylation in the accumulation of Myo2.** (A) Extract from asynchronous cells expressing HA-Myo2Ct (induced for 16 h) was prepared, and HA-Myo2Ct was immunoprecipitated using anti-HA antibodies. A half of the immunoprecipitates was treated with calf intestine alkaline phosphatase (CIAP) and the other was treated with heat-inactivated CIAP. Samples were analyzed by SDS-PAGE followed by immunoblotting using anti-HA antibodies. (left lane) Proteins of whole cell extract. (middle lane) HA-Myo2Ct immunoprecipitates that had been treated with CIAP. (right lane) HA-Myo2Ct immunoprecipitates that had been mock-treated. (A–C) Top asterisk indicates a slower migrating HA-Myo2Ct and bottom asterisk indicates a faster migrating one. (B) S1444 is a site for phosphorylation that contributes to the mobility shift on SDS-PAGE. Asynchronous cells expressing HA-Myo2Ct (lane S), HA-Myo2Ct S1444A (lane A), or HA-Myo2Ct S1444D (lane D) were grown as in A. Extracts were prepared and proteins were analyzed by SDS-PAGE followed by immunoblotting using anti-HA antibodies. (C) Phosphorylation state of S1444 within HA-Myo2Ct from G2 to mitosis. *cdc25-22* cells expressing HA-Myo2Ct (induced for 15 h) were synchronized at G2, and then released as in Fig. 2. Extracts were prepared from the G2-arrested cells (0 min) as well as those released from the arrest (20 and 40 min). Proteins were analyzed by SDS-PAGE followed by immunoblotting using anti-HA antibodies. (D) Phenotype of *myo2*Δ cells expressing HA-Myo2 S1444A and those expressing HA-Myo2 S1444D. *myo2*Δ cells expressing Myo2 S1444A (top) were grown at 30°C. *myo2*$^+$/*myo2::ura4*$^+$ diploid cells expressing HA-Myo2 S1444D were induced to undergo meiosis in a liquid medium, and spores were inoculated into a medium where only those bearing the *myo2::ura4*$^+$ allele could germinate (bottom). Both cells were fixed and stained simultaneously with anti-HA antibodies (red), Bodipy-phallacidin (green), and DAPI (blue). (E) Localization of Myo2 S1444A in G2-arrested *cdc25-22* cells. *cdc25-22* cells or *cdc25-22* cells expressing Myo2 S1444A under control of the native *myo2* promoter were grown at 25°C and shifted to 37°C for 4.5 or 5.0 h. These cells were fixed and stained simultaneously with anti-HA antibodies (right) and Bodipy-phallacidin (left). (F) Localization of HA-Myo2Ct S1444A or HA-Myo2Ct S1444D in G2-arrested *cdc25-22* cells. *cdc25-22* cells carrying construct for expression of HA-Myo2Ct S1444A (left) or HA-Myo2Ct S1444D (right) were simultaneously induced for 16 h and synchronized at G2 as in Fig. 2. These cells were fixed and stained simultaneously with anti-HA antibodies (red) and Bodipy-phallacidin (green). Bars, 3.3 μm.

dephosphorylated form (Fig. 4 B). In contrast, HA-Myo2Ct S1444D that mimics a phosphorylated form migrated at the position of the phosphorylated form (Fig. 4 B). Treatment with phosphatase or inactivated one did not affect the band pattern of the mutated HA-Myo2Cts (unpublished data). These results suggest that S1444 is the phosphorylation site that contributes to the mobility change upon SDS-PAGE. To examine whether or not phosphorylation state of S1444 changes during mitosis, we performed immunoblotting on extracts from synchronized *cdc25-22* cells expressing HA-Myo2Ct (Fig. 4 C). HA-Myo2Ct migrated as both the phosphorylated and dephosphorylated forms during G2-arrest. At 40 min after the release, HA-Myo2Ct was predominantly in the dephosphorylated form. HA-Myo2Ct in the extract of arrested *cdc10* cells was predominantly found as the phosphorylated form on SDS-PAGE (unpublished data). Thus, it is suggested that dephosphorylation of HA-Myo2Ct is promoted during early mitosis.

To investigate the role of S1444 phosphorylation, HA-Myo2 S1444A or HA-Myo2 S1444D was expressed in the *myo2*Δ cells. Cytokinesis defect in the *myo2*Δ strain was suppressed by expression of HA-Myo2 S1444A but not by that of HA-Myo2 S1444D (Fig. 4 D). HA-Myo2 S1444A localized at the CR in the *myo2*Δ cells, whereas HA-Myo2 S1444D failed to accumulate at the expected division site in these cells (Fig. 4 D). Myo2 S1444A-expressing cells tended to be round and shorter than wild-type cells; they underwent septation at a length of 7.5 μm in average, approximately half the length of the wild-type cells (Fig. 4 D). Neither anucleate nor mononucleate septated cells were observed (Fig. 4 D).

The finding that dephosphorylation of S1444 is promoted during early mitosis raised a possibility that expression of dephosphorylated form of Myo2 may cause some defect in interphase cells. To test this possibility, we examined localization of Myo2 S1444A and F-actin during interphase. *cdc25-22* cells in which the gene encoding Myo2 S1444A was integrated into the *myo2* locus were synchronized at G2 by incubating at 37°C for 4.5 h. In 48% of these cells, Myo2

S1444A accumulated as multiple dots at the medial cortex, and accumulation of F-actin cables were also seen there (Fig. 4 E). In 46% of the cells incubated at 37°C for 5 h, both Myo2 S1444A and F-actin cables were seen as a ring structure at the medial cortex (Fig. 4 E). In contrast, neither wild-type Myo2 nor F-actin cables accumulated at the medial cortex in nontransformed cells incubated at 37°C for 5 h (Fig. 4 E). Thus, it is suggested that dephosphorylation of S1444 plays an important role in promoting accumulation of Myo2 and F-actin at the division site.

Next, to investigate effects of S1444 phosphorylation on the Myo2Ct region, we examined localization of either HA-Myo2Ct S1444A or HA-Myo2Ct S1444D in G2-arrested *cdc25-22* cells. Either of the mutant proteins accumulated at the medial cortex of the G2-arrested cells (Fig. 4 F), suggesting that the Myo2Ct region has the ability to localize at the division site regardless of the phosphorylation state at S1444.

It has been reported (Mulvihill et al., 2001) that activity of Cdc7 kinase, which is a component of septum initiation network (Balasubramanian et al., 2000; McCollum and Gould, 2001), and phosphorylation at S1518 of Myo2 are required for targeting Myo2 to the CR. In contrast, Wu et al. (2003) showed that GFP-tagged Myo2 form the medial ring in the absence of Cdc7 activity. We also confirmed that GFP-tagged Myo2 could form the medial ring in the *cdc7-24* mutant cells incubated at the restrictive temperature of 36°C (unpublished data). Next, we investigated significance of phosphorylation at S1518. We created strains in which the endogenous *myo2* gene was replaced with either *myo2 S1518A* or *myo2 S1518E* (Fig. 5 A). Each mutant cells were viable at all temperatures tested, and immunolocalization experiments revealed that either Myo2 S1518A or Myo2 S1518E was recruited to the CR (Fig. 5 B). These results indicated that neither Cdc7 activity nor phosphorylation at S1518 of Myo2 is required for accumulation of Myo2 at the division site.

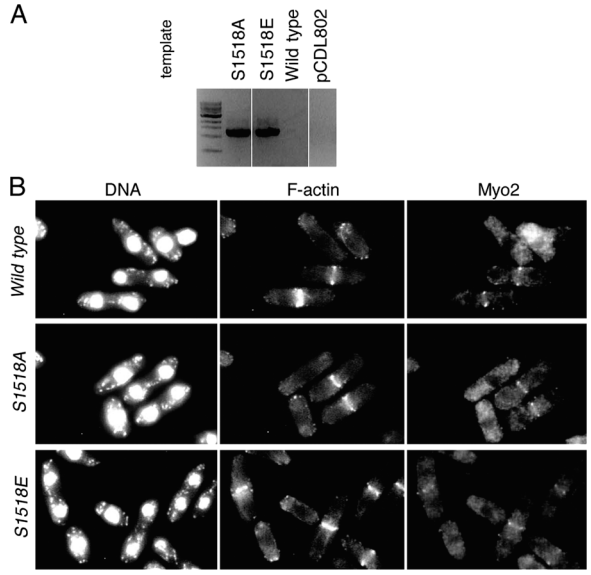

Figure 5. **Phosphorylation at S1518 of Myo2 is dispensable for the Myo2 accumulation.** (A) PCR confirmation of the myo2 S1518A and myo2 S1518E mutants. The strains integrated with the mutant gene gave a 1.25-Kb band, whereas the wild-type strain or the strain integrated with the vector only did not give this band. (B) Immunolocalization of Myo2 S1518A and Myo2 S1518E. Cells of the indicated genotypes were grown at 30°C, shifted up to 36°C, fixed, and stained with antibodies against Myo2 (right), rhodamine-phalloidin (middle), and DAPI (left).

Mid1 is required for initial accumulation of Myo2 at the division site

Because Mid1 forms multiple dots at the medial cortex in interphase cells, we compared distribution of Mid1 and that of Myo2. Mid1 was localized to the nucleus and to the medial cortex in early mitotic cells (Fig. 6 A). Myo2 colocalized with Mid1 in the medial cortex (Fig. 6 A). Thus, we investigated a role of Mid1 in the accumulation of Myo2 at the division site.

First, we analyzed localization of Myo2Ct in *mid1*Δ cells. Myo2Ct-YFP was expressed in either *mid1*Δ *cdc25-22* or *cdc25-22* cells. Although 86% of the G2-arrested *cdc25-22* cells showed accumulation of Myo2Ct-YFP at the medial cortex, no specific localization of Myo2Ct-YFP was seen in the G2-arrested *mid1*Δ cells (Fig. 6 B). It was confirmed by immunoblotting that expression level of Myo2Ct-YFP in the *mid1*Δ cells was similar to that in the control cells (unpublished data). These results indicate that Mid1 is required for the accumulation of Myo2Ct at the medial cortex.

Next, we asked whether or not accumulation of the Myo2 dots at the medial cortex occurs in the absence of Mid1. We monitored dynamics of GFP-Myo2 in *mid1*Δ *myo2*Δ cells expressing GFP-Myo2 by time-lapse imaging combined with three-dimensional reconstruction. Behavior of GFP-Myo2 in the *mid1*Δ cells was clearly different from that in the wild-type cells (Fig. 6 C). In 20 of 20 cells examined, GFP-Myo2 appeared as a cortical cable structure of random orientation, but not as cortical dots overlying the nucleus. In nine cells, the GFP-Myo2 cable extended longitudinally in the cell and did not form a ring structure. In 11 cells, the GFP-Myo2 cable eventually extended in a nonorganized manner and slowly became a ring structure of variable angles at various locations in the cell. These results suggest that Mid1 is required for the dot accumulation of Myo2 at the medial cortex during early mitosis and efficient formation of the ring structure.

We analyzed kinetics of Myo2 and F-actin accumulation in the presence or absence of Mid1. In synchronized *cdc25-22* cells, Myo2 accumulated as dots at the division site slightly earlier than an F-actin aster, as described previously (Motegi et al., 2000; Fig. 6 D). However, in synchronized *mid1*Δ *cdc25-22* cells Myo2 and F-actin simultaneously accumulated as an aberrant cable (Fig. 6 D). This result raised a possibility that Myo2 and F-actin interact with each other to form the aberrant cable in the absence of Mid1. Thus, we examined if F-actin is required for Myo2 localization in the absence of Mid1. Either *mid1*Δ or wild-type cells were treated with Lat-A, which quickly depolymerizes F-actin within 5 min. In the mitotic wild-type cells treated with Lat-A, both the Myo2 dots and the ring were maintained as reported previously (Naqvi et al., 1999). In contrast, the aberrant Myo2 cable or ring in the mitotic *mid1*Δ cells was disintegrated by Lat-A (Fig. 6 E). These results indicated that Mid1 is required for maintenance of Myo2 localization at the aberrant cable or CR in the absence of F-actin.

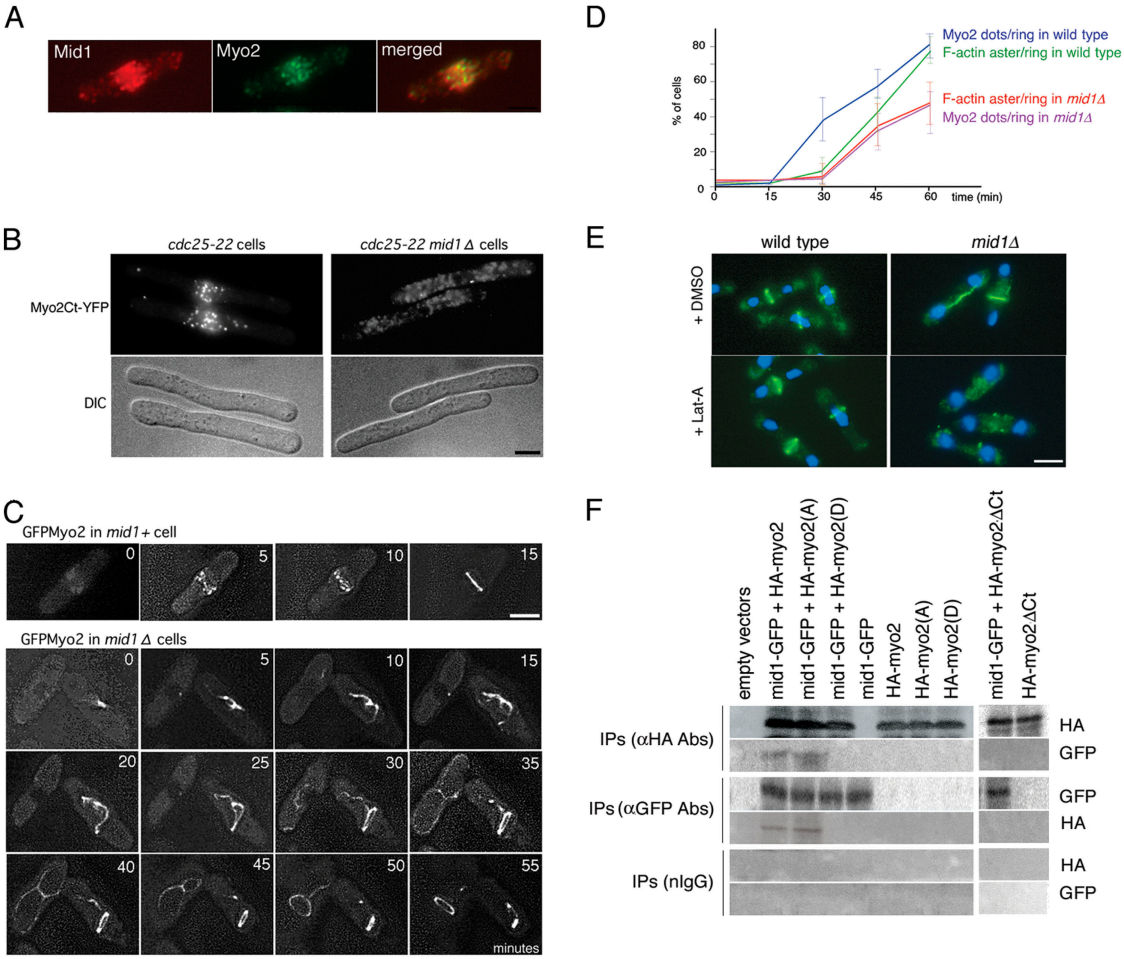

Figure 6. **Role of Mid1 in the accumulation of Myo2 at the division site.** (A) Localization of Myo2 and Mid1 in wild-type cell. Wild-type cells were simultaneously stained with anti-Mid1 antibodies (red) and anti-Myo2 antibodies (green). Strong background of anti-Mid1 staining at the medial region is due to nuclear staining. (B) Localization of Myo2Ct-YFP in G2-arrested *cdc25-22 mid1*Δ cells. *cdc25-22* cells carrying construct for expression of Myo2Ct-YFP (left) and *cdc25-22 mid1*Δ cells carrying the same construct (right) were simultaneously induced for 16 h and synchronized at G2 as in Fig. 2. Fluorescence images of Myo2Ct-YFP in live cells (top) and DIC images of these cells (bottom) were observed. Bar, 3.3 μm. (C) Dynamics of GFP-Myo2 in *mid1*Δ cells. *myo2*Δ cells expressing GFP-Myo2 (top) and *myo2*Δ *mid1*Δ cells expressing GFP-Myo2 (bottom) were observed by four dimensional imaging. Numbers indicate time in minutes. Bar, 3.3 μm. (D) Kinetics of Myo2 accumulation at the division site in *cdc25-22* cells and *mid1*Δ *cdc25-22* cells. Either *cdc25-22* cells or *mid1*Δ *cdc25-22* cells were arrested at G2, and then released by temperature shift. Localization of endogenous Myo2 was analyzed by immunofluorescence microscopy using anti-Myo2 antibodies at 15-min intervals after the release from the G2 arrest. (E) F-actin is required for retention of Myo2 at the CR in *mid1*Δ cells. Either wild-type or *mid1*Δ cells were cultured at 30°C and split into two. Lat-A was added to one half, while DMSO was added to the other. The cells were incubated for 10 min, and then fixed and stained simultaneously with DAPI (blue) and anti-Myo2 antibodies (green). Disassembly of F-actin in Lat-A–treated cells was confirmed by staining with rhodamine-phalloidin (not depicted). Bar, 3.3 μm. (F) Physical interaction between HA-Myo2 and Mid1-GFP. Extracts of cells expressing both Mid1-GFP and either HA-Myo2, HA-Myo2 S1444A (HA-Myo2, A), HA-Myo2 S1444D (HA-Myo2, D), or HA-Myo2ΔCt and those expressing either Mid1-GFP, HA-Myo2, HA-Myo2 S1444A, HA-Myo2 S1444D, or HA-Myo2ΔCt were prepared, and were immunoprecipitated with anti-HA antibodies, anti-GFP antibodies, or normal IgG. Immunoprecipitates were analyzed by SDS-PAGE followed by immunoblotting using both anti-GFP antibodies and anti-HA antibodies.

Finally, we tested whether or not Mid1 is physically associated with Myo2 in vivo. We were unable to prove the physical interaction between endogenous Myo2 and Mid1 by immunoprecipitation experiments because endogenous Mid1 was mostly present in a fraction insoluble in either detergent or high salt solution. Thus, we created a strain in which both Mid1-GFP and HA-Myo2, HA-Myo2 S1444A, HA-Myo2 S1444D, or HA-Myo2ΔCt were expressed under the *nmt1* promoter. Mid1-GFP was coimmunoprecipitated using anti-HA antibodies from the extract of cells expressing HA-Myo2 or HA-Myo2 S1444A but not from that of cells expressing HA-Myo2 S1444D or HA-Myo2ΔCt (Fig. 6 F). HA-Myo2 or HA-Myo2 S1444A, but neither HA-Myo2 S1444D nor HA-Myo2ΔCt, was coimmunoprecipitated using anti-GFP antibodies from the extracts. Neither of the proteins was detected in the immunoprecipitates using normal IgG. This result suggested that HA-Myo2 associates with Mid1-GFP through the Myo2Ct region when S1444 is dephosphorylated.

Discussion

After the onset of mitosis, Myo2 accumulates as multiple dots at the medial cortex independently of F-actin, and these dots

coalesce into a ring in an F-actin–dependent manner (Motegi et al., 2000). We identified a specific region within Myo2 for the initial accumulation. A COOH-terminal region of Myo2 consisting of 134 aa (Myo2Ct) is necessary and sufficient for the accumulation in the absence of the wild-type protein. Overexpression of Myo2Ct fragment inhibited formation of the medial F-actin ring and cytokinesis and caused formation of a medial F-actin spot from which F-actin cables emanated. Because an asterlike structure of F-actin cables has been observed during the early step of CR formation in wild-type cells (Arai and Mabuchi, 2002), it is likely that overexpressed Myo2Ct inhibits maturation of the F-actin ring from the aster. One possible mechanism for this inhibition is occupation of Myo2 target sites on the cortex by HA-Myo2Ct, which leads to interference with normal function of Myo2 to construct the CR. The other is sequestration by Myo2Ct of some factor, which is necessary for this step. A possible candidate for such factor is IQGAP Rng2 because *rng2*Δ cells form a medial spot structure of F-actin (Eng et al., 1998).

Interestingly, Myo2Ct accumulates at the future division site in early G2 cells, whereas either intact Myo2 or the tail region accumulates there after initiation of mitosis. These results suggest that the site for the Myo2 accumulation is present at the cortex from early G2 to mitosis, whereas timing of the accumulation is negatively controlled by modification of the tail region.

Myo2Ct fragment showed a mobility change on SDS-PAGE, which seemed to be due to its phosphorylation/dephosphorylation. HA-Myo2Ct S1444A or HA-Myo2 S1444D migrated at the position of the dephosphorylated or phosphorylated form, respectively, suggesting that S1444 is the in vivo phosphorylation site responsible for the mobility change. Because the dephosphorylated form of HA-Myo2Ct increased during early mitosis, we consider that it is the dephosphorylated form of Myo2 that is able to accumulate at the division site. Consistent with this hypothesis, Myo2 S1444A accumulated at the medial cortex in both G2 and mitotic cells, whereas Myo2 S1444D did not. Although we cannot exclude a possibility that Myo2 S1444D was misfolded in the cell, we do not think it is the case because Myo2Ct S1444D could localize to the division site, suggesting that the S1444D substitution did not alter the structure of this region. These results indicate that regulation of S1444 is important for the Myo2 localization, although there might be other phosphorylation sites within Myo2 involved in the regulation. Thus, it is likely that the initial step of the Myo2 accumulation is suppressed by phosphorylation at S1444 during interphase and is released by dephosphorylation during early mitosis. Although Myo2 S1444A-expressing cells were short and round, cell cycle, timing of cytokinesis, and localization of both Myo2 and F-actin were normal. Further analysis will be required to address how expression of Myo2 S1444A affects cell morphology.

How does phosphorylation/dephosphorylation at S1444 negatively control the Myo2 accumulation? The Myo2Ct fragment has the ability to localize at the division site regardless of the phosphorylation state at S1444. The fact that HA-Myo2t accumulates at the division site during mitosis, but not during interphase, suggests that the NH_2-terminal region of the tail (Myo2Nt) prevents the Myo2Ct region from targeting to the medial cortex during interphase. However, overexpression of Myo2Nt fragment neither inhibited the accumulation of HA-Myo2Ct nor suppressed lethality of cells overexpressing HA-Myo2Ct. These findings lead us to speculate that a specific conformation of the Myo2 tail is necessary to suppress targeting of Myo2Ct during interphase. Thus, we propose a model for the temporal control of the Myo2 accumulation (Fig. 7 A). Because a boundary between Myo2Nt and Myo2Ct is predicted to form a β-turn structure (Chou and Fasman, 1978), the interphase Myo2 tail may bend at the boundary. Consequently, the Myo2Ct region may be masked by an upstream region. After the onset of mitosis, signals including dephosphorylation of S1444 induce a conformational change of the tail that releases the Myo2Ct region, and thereby Myo2 can access to the division site.

All nonmuscle myosin-II heavy chains studied so far possess both a hinge region and sites for phosphorylation near the COOH terminus (for review see Tan et al., 1992). *D. discoideum* myosin has a bent at the hinge region located near the COOH terminus (Pasternak et al., 1989), and phosphorylation at three COOH-terminal sites promotes bending of the tail, and thereby inhibits assembly into filaments (Egelhoff et al., 1993; Liang et al., 1999). Because

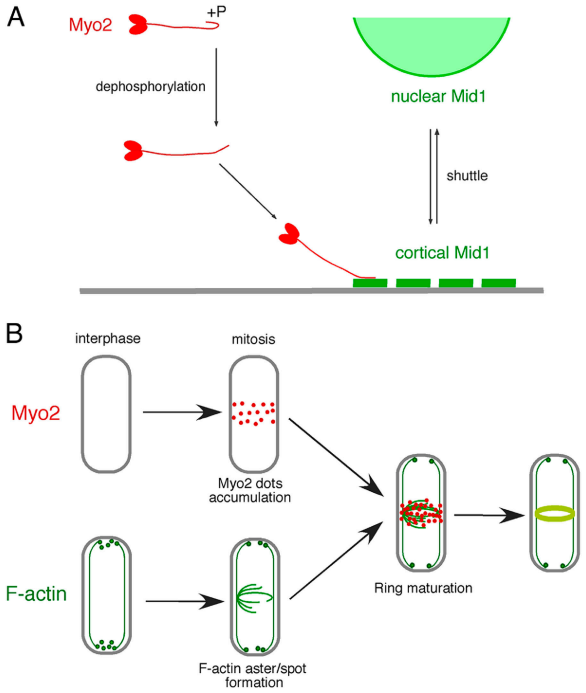

Figure 7. **Model of Myo2 accumulation at the division site.** Mid1 shuttles between the nucleus and the cortex near the nucleus from interphase to early mitosis. During interphase, phosphorylation of Myo2 S1444 suppresses Myo2 to interact with Mid1 through concealing the Myo2Ct region within its conformation. After the onset of mitosis, dephosphorylation promotes an exposure of the Ct region, and then Myo2 accesses to Mid1 at the cortex overlying the nucleus. (B) Myo2 initially accumulates as dots in a manner dependent of Mid1 and independent of F-actin. F-actin initially accumulates as an aster/spot structure at the medial cortex independently of Myo2. Then, the Myo2 dots recruit and/or stabilize F-actin cables at the medial cortex and vice versa. Finally, cortical networks of Myo2 and F-actin cables are packed into a ring through an actomyosin motor activity.

myosin localization at the cleavage furrow of amoeba requires the ability to form bipolar filaments (Sabry et al., 1997), changes in the phosphorylation state play important roles in both filament assembly and localization at the division site. Therefore, it is likely that regulation of myosin by phosphorylation/dephosphorylation is conserved among various organisms. Because we could not find any consensus sequence around S1444 of Myo2 among myosin heavy chains and any known protein kinase that exhibits consistent preference for S1444, we do not know whether the Ser residue of Myo2 is conserved or not among myosins.

What is the spatial cue for the Myo2 accumulation? The protein known so far to accumulate at the future division site is Mid1, which has been known to be required for proper positioning of the CR (Chang et al., 1996; Sohrmann et al., 1996). Our observations suggest that the initial accumulation of Myo2 via the Myo2Ct region is dependent on Mid1. First, Myo2Ct-YFP failed to accumulate at the medial cortex of the G2-arrested *mid1*Δ cells, whereas it did in the presence of Mid1. Second, GFP-Myo2 did not assemble into dots at the medial cortex in the mitotic *mid1*Δ cells. Finally, HA-Myo2 immunoprecipitated with Mid1-GFP, and the Myo2Ct region is necessary for this association. Thus, it is very likely that Mid1 associates with Myo2 through the Myo2Ct region. Furthermore, Mid1-GFP was coimmunoprecipitated with HA-Myo2 S1444A, but not with HA-Myo2 S1444D, suggesting that phosphorylation at S1444 of Myo2 inhibits the interaction with Mid1. Because position of the cortical localization of Mid1 is determined by the nucleus (Paoletti and Chang, 2000), dephosphorylation at Myo2 S1444 will recruit Myo2 at the cortex overlying the nucleus where Mid1 localizes (Fig. 7 A). Mid1 shows a similarity to anillin that has been identified in both *Drosophila melanogaster* (Field and Alberts, 1995) and human (Oegema et al., 2000) and functions in cytokinesis. It will be of interest to investigate whether or not the mechanism of myosin localization proposed here is universal among other organisms.

In spite of the absence of Mid1, Myo2 slowly formed an abnormal ring in *mid1*Δ cells. This abnormal Myo2 ring disintegrated when F-actin was disassembled, in contrast to the Myo2 ring in the wild-type cells. These results suggest that process of Myo2 localization at the division site consists of two steps: the initial accumulation depends on Mid1, and then Myo2 interacts with F-actin to form the ring in which Myo2 is stabilized by both Mid1 and F-actin (Fig. 7 B). In addition, premature accumulation of Myo2 S1444A to the division site promoted formation of F-actin ring in interphase cells. Because myosin is able to assemble F-actin of opposite polarities in vitro (Hayashi et al., 1977), Myo2 anchored at the medial cortex may be able to organize F-actin by direct interaction with F-actin. Because F-actin seems to form the asterlike structure in a manner independent of Myo2 (Motegi et al., 2000), it could be that F-actin assembly into the CR consists of two pathways, one dependent and the other independent of Myo2 (Fig. 7 B).

It is an important subject to uncover upstream signals for the control of Myo2 localization during mitosis. It has been reported that Cdc7 kinase and phosphorylation at S1518 of Myo2 is required for targeting Myo2 to the CR (Mulvihill et al., 2001). In contrast, we and others (Wu et al., 2003) showed that *cdc7* mutant cells could form a medial Myo2 ring. Moreover, we confirmed that both Myo2 S1518A and Myo2 S1518E were functional and could localize to the CR. Thus, we do not favor a model in which Cdc7 is involved in the initial accumulation of Myo2 by phosphorylating Myo2 S1518. Among the proteins essential for cytokinesis, two proteins, Cdc15 (Fankhauser et al., 1995) and Plo1 (Ohkura et al., 1995), have been known to induce CR formation in G2 cells when overexpressed. Thus, it could be that Cdc15, Plo1, or both mediate the pathway for the Myo2 accumulation. Further experiments are necessary to clarify relationships between Myo2, Plo1, and Cdc15.

Materials and methods

Strains and genetic techniques

The *S. pombe* strains used in this paper are listed in Table I. The *dmf1-ΔF* and *ssp1*Δ strains were provided by V. Simanis (The Swiss Institute for Experimental Cancer Research, Epalinges, Switzerland) and I. Rupes (Queen's University, Ontario, Canada), respectively. Standard procedures for *S. pombe* genetics were used (Moreno et al., 1991). Thiamine was used at 5 μM to repress expression from the *nmt1* promoter (Maundrell, 1989).

Table I. **Strains used in this paper**

Strain	Genotype	Reference/Source
JY1	h^- wild type	Lab stock
JY741	*ade6-216 leu1-32 ura4-D18* h^-	Lab stock
JY746	*ade6-216 leu1-32 ura4-D18* h^+	Lab stock
leu1-32	*leu1-32* h^-	Lab stock
PN1419	*cdc25-22 leu1-32 ade6-210* h^-	Russell and Nurse (1986)
JX572	*myo2*$^+$*/myo2::ura4*$^+$ *ade6-216/ade6-210 leu1-32/leu1-32 ura4-D18/ura4-D18* h^{90}/h^{90}	Kitayama et al. (1997)
JB41	*mid1-ΔF ade6-216 leu1-32 ura4-D18* h^-	Sohrmann et al. (1996)
FM202[a]	*myo2::ura4*$^+$ *ade6-216 leu1-32 ura4-D18* h^-	Motegi et al. (2000)
FM204	*cdc25-22 ura4-D18* + gene for Myo2 (S1444A) integrated	This paper
FM205[a]	*mid1-ΔF myo2::ura4*$^+$ *cdc25-22 ade6-216 leu1-32 ura4-D18* h^-	This paper
FM206[a]	*mid1-ΔF myo2::ura4*$^+$ *ade6-216 leu1-32 ura4-D18* h^-	This paper
AP46	*ade6-M210 ura4-D18 leu1-32 mid1-GFP::kan MX* h^-	Paoletti and Chang (2000)

[a]Strains FM202, FM205, and FM206 were kept as transformants.

Protein extraction, immunoprecipitation, and CIAP treatment

Protein extracts were prepared in the NP-40 buffer as described by McCollum et al. (1995). The immunoprecipitation experiment was performed as described previously (Motegi et al., 2000). For immunoblotting experiments, proteins were subjected to SDS-PAGE, and then transferred onto a polyvinylidene difluoride membrane (Millipore). This membrane was probed with antibodies against Myo2 (Motegi et al., 2000), Cdc4 (McCollum et al., 1995), α-tubulin (Sigma-Aldrich), HA, or GFP (Santa Cruz Biotechnology, Inc.), followed by detection using secondary antibodies coupled to peroxidase.

HA-Myo2Ct in the extract from cells expressing HA-Myo2Ct was immunoprecipitated, and then split into two. A half was washed twice with CIAP buffer (0.1 M Tris-HCl, pH 9.6, 2 mM $MgCl_2$, 0.1 mM $ZnCl_2$, and protease inhibitor cocktail described by Motegi et al., 2000), resuspended in 10 μl CIAP buffer containing 10 U of CIAP (Takara Shuzo), and incubated at 37°C for 15 min. The reaction was stopped by the addition of SDS-gel loading buffer followed by boiling for 3 min. The other half was mock treated. The immunoprecipitates were washed twice with CIAP buffer plus 15 mM EGTA, 5 mM NaF, and 60 mM β-glycerophosphate and resuspended in 10 μl of the same buffer containing 10 U of CIAP that had been heat treated at 75°C for 10 min (modified from Fankhauser et al., 1995).

DNA manipulations

To express a series of Myo2 truncates, DNA fragments encoding Myo2t, Myo2Nt, Myo2Ct, and Myo2ΔCt were made by PCR against plasmid pUC119-myo2 with primers pT1f (5′-CCCATATGCGATTGAAGGACATACAAGCC-3′) and pT4r (5′-CCGGATCCTCATGCGGCGCGCAACTC-3′), pT1f and pT2r (5′-CCGGATCCTCATTTCAAAACGGGTTCCG-3′), or pT3f (5′-CCCATATGAAAGCATCTAAGGTTCCCG-3′) and pT4r, respectively. The forward primers (pT1f and pT3f) contained an NdeI site, and the reverse primers (pT2r and pT4r) contained an in-frame stop codon and a BamHI site, respectively. The amplified PCR fragments were cloned into the vector pUC18 at the NdeI-BamHI sites, and then sequenced. The fragment encoding either Myo2t, Myo2Nt, or Myo2Ct was excised from the plasmid and cloned between the NdeI and BamHI sites of pHA1, an HA-tagging vector that carries the normal *nmt1* promoter, one copy of HA, and *LEU2* marker gene, yielding plasmid pLH1-m2t, pLH1-m2Nt, or pLH1-m2Ct, respectively. To replace the marker gene of the plasmid from *LEU2* to *ADE2*, the plasmid was digested with PstI and SmaI and cloned between the PstI and SmaI sites of pREP102 that carries the *ADE2* gene, yielding plasmid pAH1-m2t, pAH1-m2Nt, or pAH1-m2Ct, respectively.

For mutating S1444 in Myo2, in vitro mutagenesis was performed using the Quickchange Kit (Stratagene) and the plasmid pUC119-myo2 as a template. Point mutations were introduced according to the manufacturer's instruction using the following primers: pSAf (5′-GGGGCCGAAGTAGCACCTCAACCTACTGGC-3′) for S1444A, and pSDf (5′-GGGGCCGAAGTAGATCCTCAACCTACTGGC-3′) for S1444D, together with corresponding reverse primers. Mutated plasmids were amplified in bacteria, and the mutations were confirmed by sequencing. Either Myo2Ct with a mutation S1444A or that with S1444D was made by PCR against the mutated plasmid with primers pT3f and pT4r, and the amplified fragment was cloned into pHA1 as described in the previous paragraph. To obtain a mutant strain with a mutation for S1444A in the chromosomal *myo2* locus, a BamHI fragment was isolated from the mutated plasmid and cloned into the BamHI site of pUC18 that carries the *ura4*$^+$ cassette. The resultant plasmid was linearized and the wild-type *S. pombe* strain was transformed with it.

To express a Myo2Ct-YFP fusion protein, both NdeI and SalI sites were created at the 5′ and 3′ ends of a fragment encoding Myo2Ct, respectively, with removal of the stop codon. The *myo2*-coding region was cloned between NdeI and SalI sites of pREP1. The fragment encoding YFP (CLONTECH Laboratories, Inc.), at the 5′ end of which a SalI site had been introduced, was cloned into the aforementioned plasmid after digestion with SalI and SmaI, yielding plasmid pL1m2CtY. The linkage sequence between the 3′ end of *myo2* and the 5′ end of YFP-coding sequence was GTCGACCAT. The construct for expression of Mid1-GFP was provided by R. Lustig and F. Chang (Columbia University, New York, NY).

Immunofluorescence staining and microscopy

For observation of the Myo2 truncate in *myo2*Δ cells, each Myo2 truncate tagged at the NH_2 terminus with HA epitope was expressed in *myo2*$^+$/*myo2::ura4*$^+$ diploid strain JX572. These diploid cells were sporulated, and haploid spores bearing both the *myo2::ura4*$^+$ allele and the construct were selected. Localization of the Myo2 truncates was observed in cells undergoing second mitosis after germination. For observation of the Myo2 truncates in synchronized cells, *cdc25-22* or *cdc10-V50* cells were transformed with each construct encoding the HA-tagged Myo2 truncate. The *cdc25-22* and *cdc10-V50* cells were arrested cell cycle at G2 and G1, respectively, by culturing at 37°C for 4 h. Immunoblotting experiments showed that expression level of each Myo2 truncate under control of the *nmt1* promoter increased 15 h after removal of thiamine from the medium. Thus, the mutant cells carrying the construct were cultured for 15 h in the absence of thiamine at 25°C and arrested by temperature shift to 37°C. The cells were released from the arrest by shifting the temperature to 25°C.

Cells were fixed in 3% PFA for 50 min. Immunostaining of the cells was performed as described previously (Arai et al., 1998; Motegi et al., 2000). Anti-Dmf1/Mid1 antibodies used as primary antibodies were provided by V. Simanis. Secondary antibodies used were Bodipy-conjugated anti–rabbit IgG IgG (goat), rhodamine-conjugated anti–rabbit IgG IgG (goat), or rhodamine-conjugated anti–mouse IgG IgG (goat) (Molecular Probes). F-actin was stained with Bodipy-phallacidin (Molecular Probes). Fluorescence microscopy of GFP-containing or immunostained cells were performed with a Delta Vision System (Applied Precision) using a microscope (model IX70; Olympus) equipped with UplanApo 100× objective lens at 20°C. Original images of serial optical sections were taken every 0.2 μm in the direction of the z-axis. These images were deconvoluted, reconstructed to obtain three-dimensional images, and processed with Adobe Photoshop.

We are grateful to Drs. Raymond Lustig and Fred Chang for the construct for expression of Mid1-GFP, Dr. Viesturs Simanis for the *dmf1-ΔF* strain and anti-Dmf1/Mid1 antibodies, and Dr. Ivan Rupes for the *ssp1*Δ strain. We also thank Dr. Asako Sugimoto and all members of our laboratory for encouragement and stimulating discussions.

This work was supported by a Research Fellowship of the Japan Society for the Promotion of Science for Young Scientists to F. Motegi and a special research grant from the Ministry of Education, Science, and Culture of Japan (10213202) to I. Mabuchi.

Submitted: 18 February 2004
Accepted: 27 April 2004

References

Arai, R., and I. Mabuchi. 2002. F-actin ring formation and the role of F-actin cables in the fission yeast *Schizosaccharomyces pombe*. *J. Cell Sci.* 115:887–898.

Arai, R., K. Nakano, and I. Mabuchi. 1998. Subcellular localization and possible function of actin, tropomyosin and actin-related protein 3 (Arp3) in the fission yeast *Schizosaccharomyces pombe*. *Eur. J. Cell Biol.* 76:288–295.

Bahler, J., A.B. Steever, S. Wheatley, Y. Wang, J.R. Pringle, K.L. Gould, and D. McCollum. 1998. Role of polo kinase and mid1p in determining the site of cell division in fission yeast. *J. Cell Biol.* 143:1603–1616.

Balasubramanian, M.K., D. McCollum, and U. Surana. 2000. Tying the knot: linking cytokinesis to the nuclear cycle. *J. Cell Sci.* 113:1503–1513.

Barral, J.M., A.H. Hutagalung, A. Brinker, F.U. Hartl, and H.F. Epstein. 2002. Role of the myosin assembly protein UNC-45 as a molecular chaperone for myosin. *Science.* 25:669–671.

Benzanilla, M., and T.D. Pollard. 2000. Myosin-II tails confer unique functions in *Schizosaccharomyces pombe*: characterization of a novel myosin-II tail. *Mol. Biol. Cell.* 11:79–91.

Benzanilla, M., S.L. Forsburg, and T.D. Pollard. 1997. Identification of a second myosin-II in *S. pombe*: Myp2p is conditionally required for cytokinesis. *Mol. Biol. Cell.* 8:2693–2705.

Bi, E., P. Maddox, D.J. Lew, E.D. Salmon, J.N. McMillan, E. Yeh, and J.R. Pringle. 1998. Involvement of an actomyosin contractile ring in *Saccharomyces cerevisiae* cytokinesis. *J. Cell Biol.* 142:1301–1312.

Chang, F., and P. Nurse. 1996. How fission yeast fission in the middle. *Cell.* 84: 191–194.

Chang, F., A. Woollard, and P. Nurse. 1996. Isolation and characterization of fission yeast mutants defective in the assembly and placement of the contractile actin ring. *J. Cell Sci.* 109:131–142.

Chou, P.Y., and G.D. Fasman. 1978. Prediction of the secondary structure of proteins from their amino acid sequence. *Adv. Enzymol. Relat. Areas Mol. Biol.* 47:45–148.

Egelhoff, T.T., R.J. Lee, and J.A. Spudich. 1993. *Dictyostelium* myosin heavy chain phosphorylation sites regulate myosin filament assembly and localization in vivo. *Cell.* 75:363–371.

Eng, K., N.I. Naqvi, K.C. Wong, and M.K. Balasubramanian. 1998. Rng2p, a protein required for cytokinesis in fission yeast, is a component of the actomyosin ring and the spindle pole body. *Curr. Biol.* 8:611–621.

Fankhauser, C., A. Reymond, L. Cerutti, S. Utzig, K. Hofmann, and V. Simanis. 1995. The *S. pombe* cdc15 gene is a key element in the reorganization of F-actin at mitosis. *Cell.* 82:435–444.

Field, C.M., and B.M. Alberts. 1995. Anillin, a contractile ring protein that cycles from the nucleus to the cell cortex. *J. Cell Biol.* 131:165–178.

Hayashi, T., R.B. Silver, M.L. Cayer, and D.S. Smith. 1977. Actin-myosin interaction. Self-assembly into a bipolar "contractile unit". *J. Mol. Biol.* 111: 159–171.

Kitayama, C., A. Sugimoto, and M. Yamamoto. 1997. Type II myosin heavy chain encoded by the *myo2* gene composes the contractile ring during cytokinesis in *Schizosaccharomyces pombe. J. Cell Biol.* 137:1309–1319.

Le Goff, X., S. Utzig, and V. Simanis. 1999. Controlling septation in fission yeast: finding the middle and timing it right. *Curr. Genet.* 35:571–584.

Liang, W., H.M. Warrick, and J.A. Spudich. 1999. A structural model for phosphorylation control of *Dictyostelium* myosin II thick filament assembly. *J. Cell Biol.* 147:1039–1047.

Lippincott, J., and R. Li. 1998. Sequential assembly of myosin II, an IQGAP-like protein, and filamentous actin to a ring structure involved in budding yeast cytokinesis. *J. Cell Biol.* 140:355–366.

Marks, J., and J.S. Hyams. 1985. Localization of F-actin through the cell division cycle of *Schizosaccharomyces pombe. Eur. J. Cell Biol.* 39:27–32.

Maundrell, K. 1989. nmt1 of fission yeast. A highly transcribed gene completely repressed by thiamine. *J. Biol. Chem.* 265:10857–10864.

May, K.M., F.Z. Watts, N. Jones, and J.S. Hyams. 1997. Type II myosin involved in cytokinesis in the fission yeast, *Schizosaccharomyces pombe. Cell Motil. Cytoskeleton.* 38:385–396.

McCollum, D., and K.L. Gould. 2001. Timing is everything: regulation of mitotic exit and cytokinesis by the MEN and SIN. *Trends Cell Biol.* 11:89–95.

McCollum, D., M.K. Balasubramanian, L.E. Pelcher, S.M. Hemmingsen, and K.L. Gould. 1995. *Schizosaccharomyces pombe cdc4*$^{+}$ gene encodes a novel EF-hand protein essential for cytokinesis. *J. Cell Biol.* 130:651–660.

Mitchison, J.M., and P. Nurse. 1985. Growth in cell length in the fission yeast *Schizosaccharomyces pombe. J. Cell Sci.* 75:357–376.

Moreno, S., A. Klar, and P. Nurse. 1991. Molecular genetic analysis of fission yeast *Schizosaccharomyces pombe. Methods Enzymol.* 194:795–823.

Motegi, F., K. Nakano, C. Kitayama, M. Yamamoto, and I. Mabuchi. 1997. Identification of Myo3, a second type-II myosin heavy chain in the fission yeast *Schizosaccharomyces pombe. FEBS Lett.* 420:161–166.

Motegi, F., K. Nakano, and I. Mabuchi. 2000. Molecular mechanism of myosin-II assembly at the division site in *Schizosaccharomyces pombe. J. Cell Sci.* 113: 1813–1825.

Mulvihill, D.P., C. Barretto, and J.S. Hyams. 2001. Localization of fission yeast type II myosin, Myo2, to the cytokinetic actin ring is regulated by phosphorylation of a C-terminal coiled-coil domain and requires a functional septation initiation network. *Mol. Biol. Cell.* 12:4044–4053.

Naqvi, N.I., K. Eng, K.L. Gould, and M.K. Balasubramanian. 1999. Evidence for F-actin-dependent and -independent mechanisms involved in assembly and stability of the medial actomyosin ring in fission yeast. *EMBO J.* 18:854–862.

Noguchi, T., and I. Mabuchi. 2001. Reorganization of actin cytoskeleton at the growing end of the cleavage furrow of *Xenopus* egg during cytokinesis. *J. Cell Sci.* 114:401–412.

Oegema, K., M.S. Savoian, T.J. Mitchison, and C.M. Field. 2000. Functional analysis of a human homologue of the *Drosophila* actin binding protein anillin suggests a role in cytokinesis. *J. Cell Biol.* 150:539–552.

Ohkura, H., I.M. Hagan, and D.M. Glover. 1995. The conserved *Schizosaccharomyces pombe* kinase plo1, required to form a bipolar spindle, the actin ring, and septum, can drive septum formation in G1 and G2 cells. *Genes Dev.* 9:1059–1073.

Paoletti, A., and F. Chang. 2000. Analysis of mid1p, a protein required for placement of the cell division site, reveals a link between the nucleus and the cell surface in fission yeast. *Mol. Biol. Cell.* 11:1603–1616.

Pasternak, C., P.F. Flicker, S. Ravid, and J.A. Spudich. 1989. Intermolecular versus intramolecular interactions of *Dictyostelium* myosin: possible regulation by heavy chain phosphorylation. *J. Cell Biol.* 109:203–210.

Rupes, I., Z. Jia, and P.G. Young. 1999. Ssp1 promotes actin depolymerization and is involved in stress response and new end take-off control in fission yeast. *Mol. Biol. Cell.* 10:1495–1510.

Russell, P., and P. Nurse. 1986. cdc25^{+} functions as an inducer in the mitotic control of fission yeast. *Cell.* 11:145–153.

Sabry, J.H., S.L. Moores, S. Ryan, J.H. Zang, and J.A. Spudich. 1997. Myosin heavy chain phosphorylation sites regulate myosin localization during cytokinesis in live cells. *Mol. Biol. Cell.* 8:2605–2615.

Schroeder, T.E., and J.J. Otto. 1988. Immunofluorescent analysis of actin and myosin in isolated contractile ring of sea urchin eggs. *Zoological Science.* 5:713–725.

Sohrmann, M., C. Fankhauser, C. Brodbeck, and V. Simanis. 1996. The dmf1/mid1 gene is essential for correct positioning of the division septum in fission yeast. *Genes Dev.* 10:2707–2719.

Tan, J.L., S. Ravid, and J.A. Spudich. 1992. Control of nonmuscle myosins by phosphorylation. *Annu. Rev. Biochem.* 61:721–759.

Wong, K.C.Y., N.I. Naqvi, Y. Iino, M. Yamamoto, and M.K. Balasubramanian. 2000. Fission yeast Rng3p: an UCS-domain protein that mediates myosin II assembly during cytokinesis. *J. Cell Sci.* 113:2421–2432.

Wu, J.-Q., J.R. Kuhn, D.R. Kovar, and T.D. Pollard. 2003. Spatial and temporal pathway for assembly and constriction of the contractile ring in fission yeast cytokinesis. *Dev. Cell.* 5:723–734.

Zang, J.H., and J.A. Spudich. 1998. Myosin II localization during cytokinesis occurs by a mechanism that does not require its motor domain. *Proc. Natl. Acad. Sci. USA.* 95:13652–13657.